Fabrication of micron-sized tetrahedra by Si⟨1 1 1⟩ micromachining and retraction edge lithography

2012 J. Micromech. Microeng. 22 085032

(http://iopscience.iop.org/0960-1317/22/8/085032)

J. Micromech. Microeng. **22** (2012) 085032 (7pp) doi:10.1088/0960-1317/22/8/085032

Fabrication of micron-sized tetrahedra by Si⟨1 1 1⟩ micromachining and retraction edge lithography

Rajeevan Kozhummal[1,2,3], Erwin Berenschot[2], Henri Jansen[2], Niels Tas[2], Margit Zacharias[1,3] and Miko Elwenspoek[1,2]

[1] School of Soft Matter Research, Freiburg Institute for Advanced Studies (FRIAS), Albert Ludwigs University of Freiburg, Albertstraße 19, D-79104 Freiburg, Germany
[2] Transducers Science and Technology (TST), MESA+ Institute for Nanotechnology, University of Twente, PO Box 217, 7500 AE, Enschede, The Netherlands
[3] Nanotechnology, Institute of Microsystems Engineering (IMTEK), Albert Ludwigs University of Freiburg, Georges-Köhler-Allee 103, D-79110 Freiburg, Germany

E-mail: rajeevan.kozhummal@frias.uni-freiburg.de

Received 19 December 2011, in final form 20 June 2012
Published 20 July 2012
Online at stacks.iop.org/JMM/22/085032

Abstract
A new method is proposed to prepare micron-sized anisotropic-shaped particles: tetrahedral structures bounded by ⟨1 1 1⟩ faces. It is based on the micromachining of ⟨1 1 1⟩-oriented silicon wafers and retraction edge lithography (REL). The size of these Si structures is tunable but limited: roughly from 20 to 2000 nm. The importance of this method is that the fabricated structure resembles almost perfectly the mathematical tetrahedron. Furthermore, the technique offers room to change the anisotropic property of the particle by selective modification of the faces using self-aligned lithography.

(Some figures may appear in colour only in the online journal)

1. Introduction

Well-defined silicon structures bounded by ⟨1 1 1⟩ planes are important in micro system technology. They find applications in e.g. optical and electronic devices, sensors and micro-electro-mechanical systems [1–3]. The possibility of tetrahedral Si particles assembling and forming crystal structures has been found to be intriguing, notably in simulation studies. In 2005, it was shown that spherical particles with patches on the surface at the corners of a tetrahedron can form a diamond-like structure by self-assembly [4]. Simulations indicate that tetrahedra pack into quasicrystals with a high packing fraction [5–7]. Tetrahedral particles have been synthesized by bottom-up as well as top-down pathways. Chemically, by using a coordinating and capping ligand, Si tetrahedra were prepared bottom-up [8]. By contrast, Berenschot *et al* reported a top-down method to machine single crystalline tetrahedral structures bound by Si ⟨1 1 1⟩ faces and outlined the prospective applications principally in self-assembly [9]. They described the preparation of tetrahedra in the range from 20 to 1000 nm. Here we report a new self-aligned strategy, which facilitates a high degree of symmetry in the particle's shape. It uses Si⟨1 1 1⟩ wafers and enables selective modification of the faces as will be demonstrated.

2. Fabrication

The strong anisotropy of etch rate among the crystallographic planes is well known in wet etching. For example, the Si etch rate in the ⟨1 1 1⟩ direction is much smaller than in the other directions for widely used etchants like KOH (potassium hydroxide), EDP (ethylene-diamine pyrocatechol) and TMAH (tetra-methyl-ammonium hydroxide) [10]. This anisotropy is often used in the fabrication of structures in Si⟨1 0 0⟩ wafers [11–14], but in the present work Si⟨1 1 1⟩ wafers will be used to fabricate tetrahedra. However, a process using photolithography to open a triangular shape along the ⟨1 1 1⟩ faces, followed by Si etching, typically would not form a tetrahedron. However, in the present study another method will

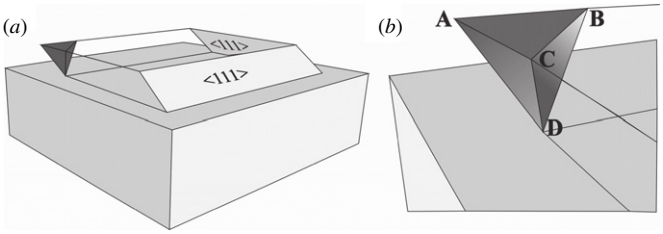

Figure 1. (*a*) Schematic representation of a tetrahedron bound by Si⟨1 1 1⟩ facets machined out of a parallelepiped structure, which is machined out of a Si⟨1 1 1⟩ wafer. (*b*) This zoom-in shows the four tips of the tetrahedron A, B, C and D. The plane described by the face ABC is part of the initial wafer surface.

be adopted to preserve sharp corners in which the three out-of-wafer plane faces of the tetrahedron are formed in a three-step process one by one. Even though this technique increases the process complexity, the advantage is that the engineer has more freedom to design and change the property of individual faces of the tetrahedron. The latter might encourage the process of self-assembly.

Wet etching of Si⟨1 1 1⟩ is generally concerned with the slow etch property of the ⟨1 1 1⟩ faces and as such will form hollow octahedral or parallelepiped features [15–17]. In the current technique, one corner of such a solid parallelepiped is machined into a tetrahedron. As shown in figure 1, the wafer surface itself forms the first face of the tetrahedron (ABC). The second and third ⟨1 1 1⟩ faces, ACD and ABD, are created sequentially by lithography and Si etching. After each stage, the newly opened Si⟨1 1 1⟩ surface is protected with silicon dioxide (SiO_2). The fourth and last face, BCD, is made by a maskless lithographic technique called retraction edge lithography (REL), which is a perfect tool for fabricating wafer-scale nanostructures precisely and controllably [18–21]. In the coming sections, the exact procedure of above is described.

2.1. Opening of the second face of the tetrahedron

This process involves Si etching using KOH through a grating mask to reveal two parallel ⟨1 1 1⟩ surfaces: A wafer (100 mm diameter p-type Si ⟨1 1 1⟩, thickness 525 μm $\pm$ 25 μm) is dry oxidized at 950 °C to grow 40 nm SiO_2. Subsequently, 70 nm of low-stress Si-rich nitride (SiN_x) is deposited by low-pressure chemical vapor deposition (LPCVD). This double layer is patterned with photoresist using a grating mask (15 μm line and 5 μm spacing) with the lines in a direction perpendicular to the wafer-flat, i.e. the grating lines are aligned with the ⟨1 1 0⟩-direction. The nitride is etched by dry etching, the resist is stripped and the oxide is etched by buffered hydrofluoric acid (BHF 1:7) for 2 min to create a double mask on Si as depicted in figure 2(*a*). Subsequently, the unprotected Si is etched for 180 min (25 wt% KOH at 75 °C) reaching a depth of 2.6 μm to open two parallel Si ⟨1 1 1⟩ surfaces on both sides of the grating pattern (figure 2(*b*)).

2.2. Opening of the third face of the tetrahedron

As shown in the process flow in figure 3, this step is to create a semiparallelepiped structure bound by Si⟨1 1 1⟩ faces: first, the KOH-patterned wafer of section 2.1 is cleaned by RCA2 and dry oxidized at 1100 °C to get 190 nm LOCOS protective oxide (local oxidation of silicon) at the just revealed ⟨1 1 1⟩ planes (figure 3(*a*)). A layer of 100 nm LPCVD poly-silicon is deposited at 590 °C (figure 3(*b*)) followed by wet oxidation at 800 °C to grow 10 nm thin oxide on top of the poly-Si layer (figure 3(*c*)). Next, the same grating pattern as before is applied, but roughly 60° rotated with respect to the initial pattern. The process is not affected by misalignment of a few degrees or more. This is because the anisotropic etch will force the shape to stop at the nearest ⟨1 1 1⟩ plane. When a mask edge is misaligned, instead of an atomically flat facet it leads to a train of steps like a staircase, where the surface of the step is atomically flat ⟨1 1 1⟩. Etching proceeds such that atoms are removed from the step edge; that means that the step moves [22, 23]. There is also a small etch rate of the ledges of the step, but the edge etches much faster. The features are etched quite deep, so that the steps due to misalignment had time to move along the lateral length of the features, so the small misalignment has no influence on the result. After the development of the resist, the unprotected oxide on the poly-Si is etched by 1% HF (figure 3(*d*)). Note that the residual resist under the roofs of the undercuts protects this thin oxide as well, because the poly-Si is opaque for the UV exposure. The resist is removed using acetone/isopropanol to prevent native oxide growth (figure 3(*e*)) and the poly-Si layer is etched by 25 wt% TMAH at 70 °C for 25 s using the oxide pattern (figure 3(*f*)). The thin oxide on top of the poly-Si pattern is stripped (figure 3(*g*)) and the exposed double layer of nitride on top of oxide is etched by H_3PO_4 at 180 °C and the oxide is etched in BHF (figures 3(*h*) and (*i*)). Next, the wafer is immersed in TMAH for 180 min to open the third ⟨1 1 1⟩ face to reach a depth of 3.2 μm (figure 3(*j*)). TMAH is chosen instead of KOH owing to its high selectivity to oxide [24, 25]. This step also strips the poly-Si layer on top of the double layer.

2.3. Opening the fourth face of the tetrahedron: retraction edge lithography (REL)

A straightforward method to form the fourth face, BCD, might be to use lithography once again to open a part of the nitride mask at the top face of the parallelepiped. However, this method is not preferred for the fabrication of small accurate structures considering the resolution and precision of lithography. Therefore, REL has been adopted as described by Zhao *et al* [18]. REL can overcome the need of an extra mask by using the already present double layer, i.e. undercutting the oxide beneath the nitride layer (figures 4 and 5(*a*)). In figure 4, the oxide pull-back underneath the edges is represented as X and θ is half the angle between two edges, i.e. 30°. From the figure, $X = L \sin\theta$ giving $L = 2X$. By varying the pull-back, the size of the tetrahedron formed can be tuned from ∼20 to 2000 nm. The size can be scaled up, as long as the nitride overhang is mechanically stable. Note that the line roughness of the double layer, derived from the lithographic procedure, is virtually removed by the forming of the ⟨1 1 1⟩ planes. These almost perfect ⟨1 1 1⟩ planes are the starting point of the retraction etching [26].

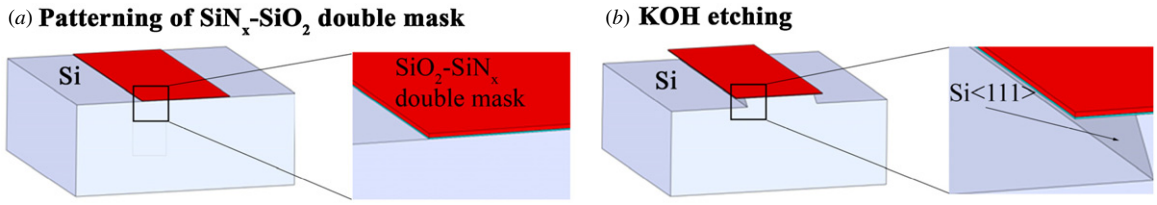

Figure 2. Schematic representation of opening the second Si⟨1 1 1⟩ face. (*a*) 70 nm nitride on top of 40 nm oxide is patterned resulting in a double mask. (*b*) Anisotropic KOH etching using the double mask opens up two Si⟨1 1 1⟩ parallel planes.

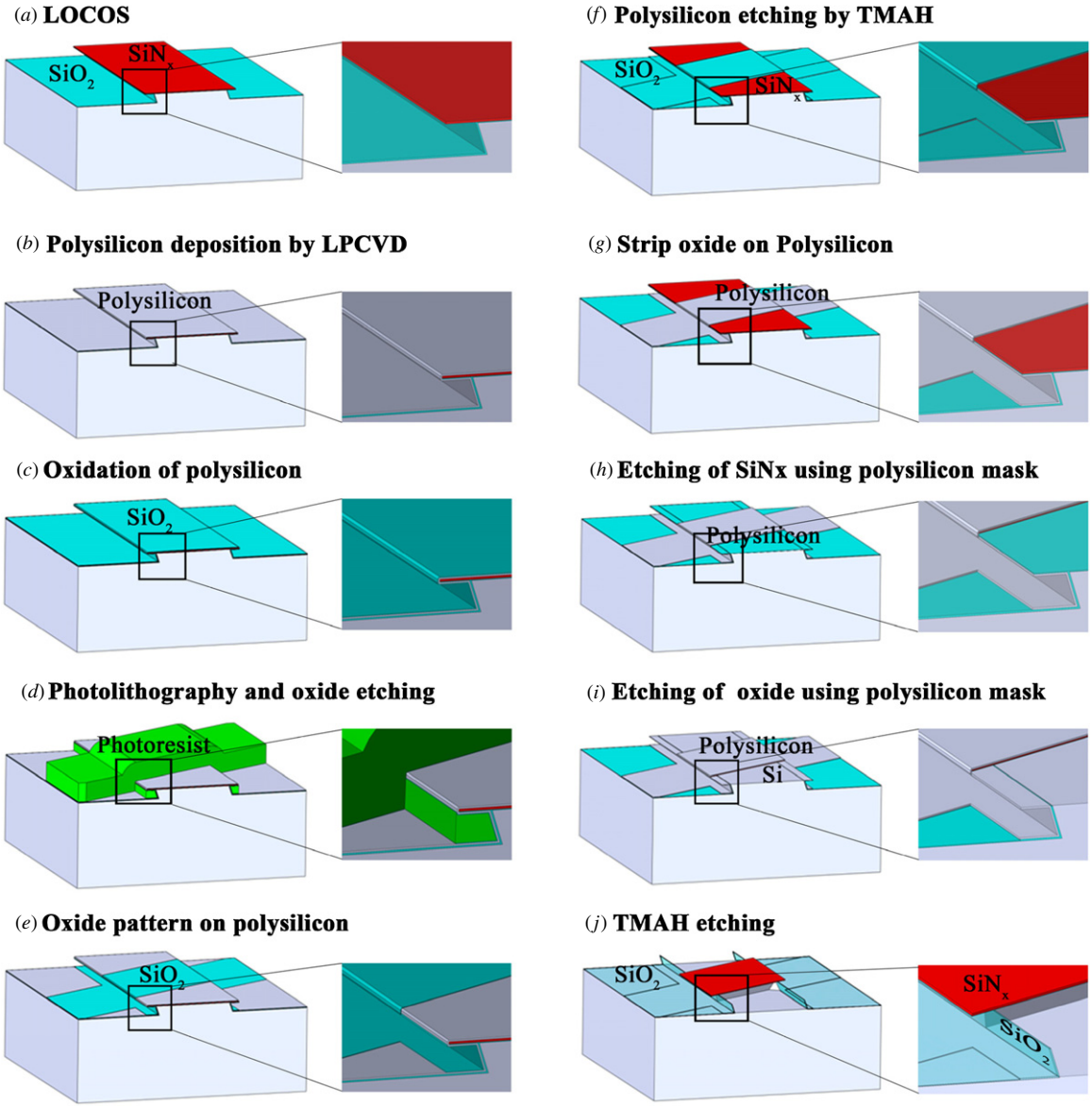

Figure 3. Schematic of the fabrication steps to reveal the third ⟨1 1 1⟩ face of the tetrahedron. (*a*) Local oxidation of Si (LOCOS). (*b*) Conformal coating with LPCVD poly-Si. (*c*) Oxidation. (*d*) Resist pattern, roughly 60° rotated to the initial pattern, and subsequent oxide etch. (*e*) Resist strip. (*f*) Wet TMAH etch of poly-Si. (*g*) Oxide strip. (*h*) Nitride etch. (*i*) The 40 nm oxide is also removed using the same mask. (*j*) TMAH etch forms the third face and it strips poly-Si.

To start this sequence, the double layer is treated with 50% HF to retract the oxide layer below the nitride (figures 4 and 5(*a*)). The etch time is adjusted to 2 min for an oxide retraction of $X \sim 2.3\ \mu$m. The nitride is etched to slightly more than half of the thickness with H_3PO_4 for the shaping of the top nitride layer (figure 5(*b*)). The overhang is removed completely in this step since it is etched at top and bottom. The wafer is cleaned and Si is wet oxidized at 1100 °C to grow 350 nm thick oxide (figure 5(*c*)). The native oxide on the nitride is removed with 1% HF and the nitride is etched with H_3PO_4 for 28 min. The 40 nm oxide from the double layer is then stripped with BHF for 50 s. This leaves the thicker oxide on the three faces

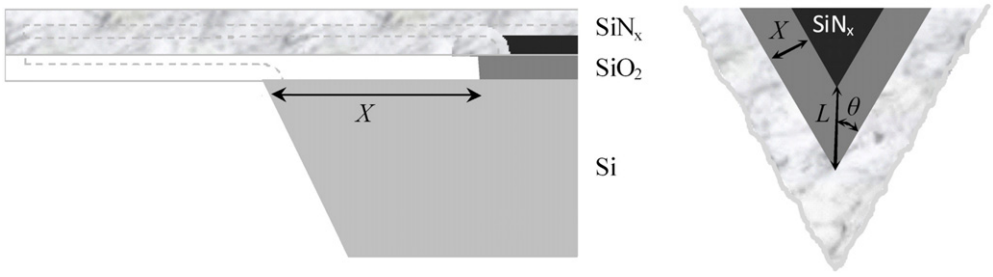

Figure 4. Top and cross sectional view of figure 5(*a*): the corner after oxide REL with nitride overhang.

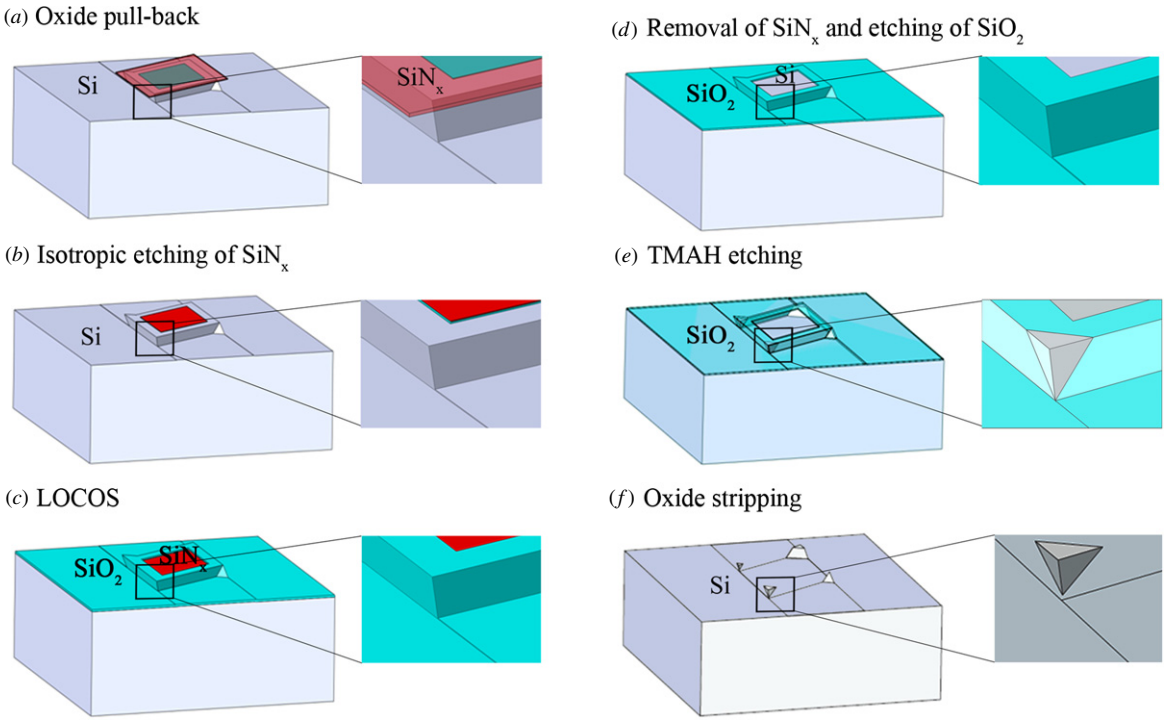

Figure 5. Schematic drawing of how to finish the tetrahedron out of the parallelepiped by REL. (*a*) Oxide retraction by HF. (*b*) Removal of the nitride overhang. (*c*) A thick oxide layer is grown. (*d*) The double layer is completely stripped leaving part of the thick oxide. (*e*) TMAH etch to get the fourth face of the tetrahedron. (*f*) Oxide strip releases the tetrahedron from the wafer.

of the corner virtually intact (figure 5(*d*)). Finally, the fourth and last ⟨1 1 1⟩ face is formed by etching with TMAH for 170 min to leave a tetrahedron at the tip of the parallelepiped (figure 5(*e*)). In order to free the tetrahedron, the oxide is etched with HF (figure 5(*f*)).

2.4. Independent patterning the first face of the tetrahedron: a self-aligned process

A big advantage of creating the faces of the tetrahedron one by one is that the faces can have different properties. This is an important feature in the process of self-assembly. In figure 6 the self-aligned patterning of the first face is demonstrated. The process description starts after shaping the final face of the tetrahedron (figures 5(*e*) and 6(*a*)). Structures with tetrahedral features of edge length 1.7 μm are used for this patterning. The drawing is rotated and the tetrahedron is cut midways for clarity (figures 6(*b*) and (*c*)). To start with, the fourth face is protected with 20 nm dry oxide. The oxide on top of the tetrahedron is removed directionally with RIE (figure 6(*d*)) [27] and the unprotected Si is subsequently etched (100 nm in 5.5 min) by TMAH (figure 6(*e*)). Then, 136 nm of LPCVD nitride is conformally deposited (figure 6(*f*)) and partly etched for 41 min by H_3PO_4 using corner lithography [28]. This leaves a nitride ring on top of the Si structure (figure 6(*g*)). An additional TMAH etching through SiN_x opening results in a tetrahedron with a silicon ridge and a nitride ring on one of the faces (figure 6(*h*)). Both the structures (figures 6(*g*) and (*h*)) are released by etching with 50% HF for 1 min (figures 8(*a*) and (*b*)). Etching with 50% HF for a longer time (15 min) strips off the nitride mask and forms modified silicon tetrahedral structures with a ridge on the top face (figures 6(*i*) and 8(*c*)).

A similar modification of the side BCD as indicated in figure 1 should be feasible before release (step f in figure 5) since the side is open. Therefore, two different sides of the tetrahedra might be modified independently.

3. Results and discussion

In the SEM image in figures 7(*a*) and (*b*), at the corner marked as O, the tetrahedron is still protected by thick oxide. But in

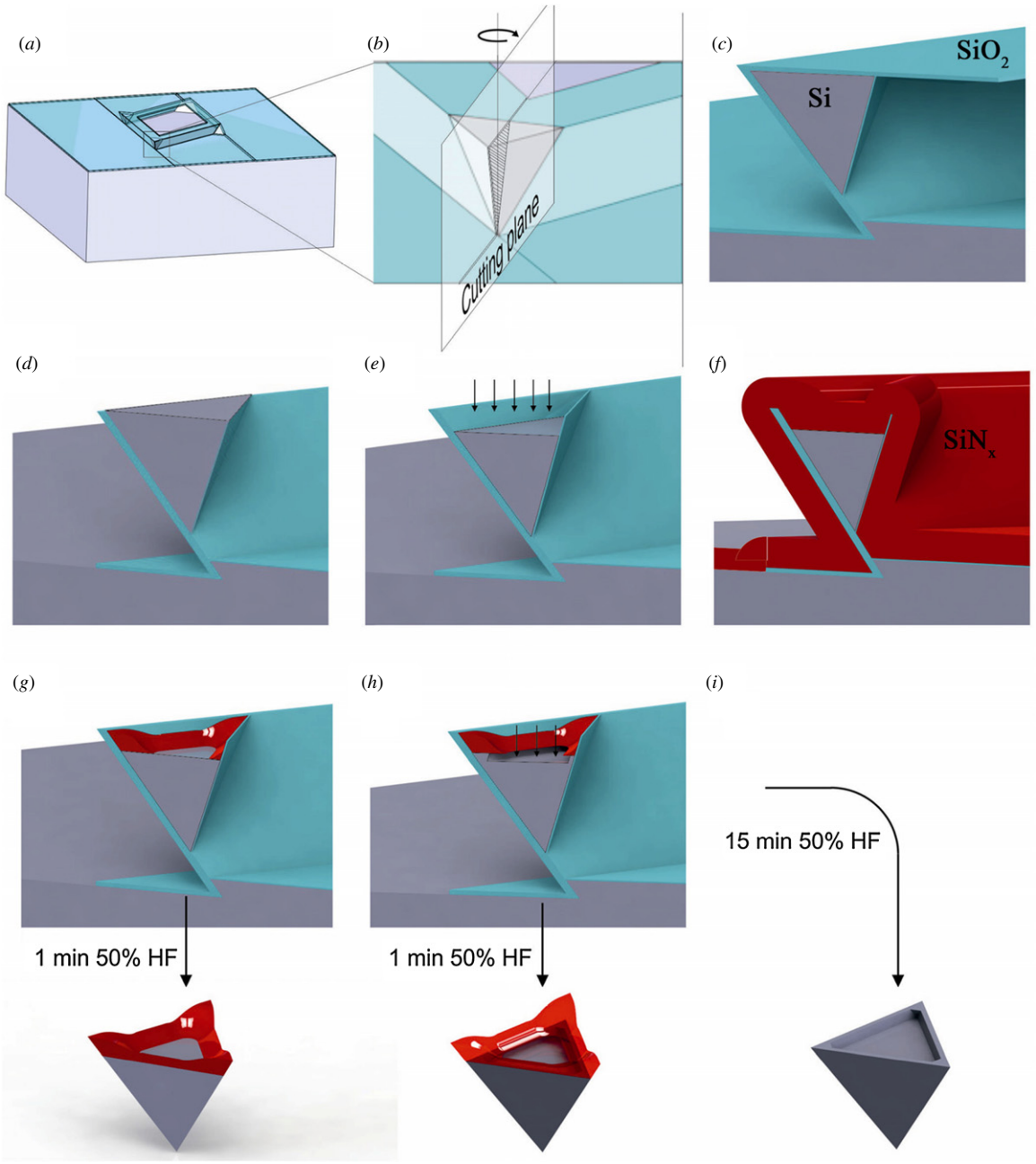

Figure 6. Self-aligned patterning of the first face of a tetrahedron: (*a*)–(*c*) Rotation and zoom-in of figure 5(*e*) for clarity, (*d*) RIE of oxide of top face, (*e*) TMAH etching, (*f*) LPCVD SiN_x and (*g*) Corner lithography of nitride. Subsequent etching in 50% HF for 1 min results in release of tetrahedron with a nitride ring is shown below. (*h*) 2 min TMAH etching through the SiN_x opening (40 nm deep). Tetrahedron releases after this step is shown below. (*i*) Tetrahedron releases by etching with 50% HF for 15 min.

figures 7(*c*) and (*d*), the tetrahedron is released by the HF. In addition to the intended tetrahedron some other structures are also produced. This includes a truncated pyramid (at the corner M), a pyramid at the corner N and a tetrahedron of smaller size at the corner P.

3.1. Effect of oxidation temperature on the shape of dry oxidized Si⟨1 1 1⟩ convex edges

The selection of an oxidation temperature, which hardly alters the morphology of the convex edge between ⟨1 1 1⟩ planes, is important in this process. The following experiment has been carried out: test structures with convex ⟨1 1 1⟩ edges are prepared (figure 9(*a*)) by etching patterned ⟨1 0 0⟩Si wafers as described by Berenschot *et al* [9]. The samples have been dry oxidized at different temperatures between 950 and 1150 °C to get around 50 nm oxide. A total of 60 nm of LPCVD poly-Si is deposited to get a better contrast for SEM observation. As observed in figure 9, the convex shape varies with temperature. For 60 min at 950 °C (figure 9(*b*)), a slightly sharpened Si edge after oxidation is formed. Successively less sharpening is observed for 40 min at 1000 °C (figure 9(*c*)), for 24 min at 1050 °C (figure 9(*d*)) and for 12 min at 1100 °C (figure 9(*e*)). For 8.5 min at 1150 °C the edge starts to round

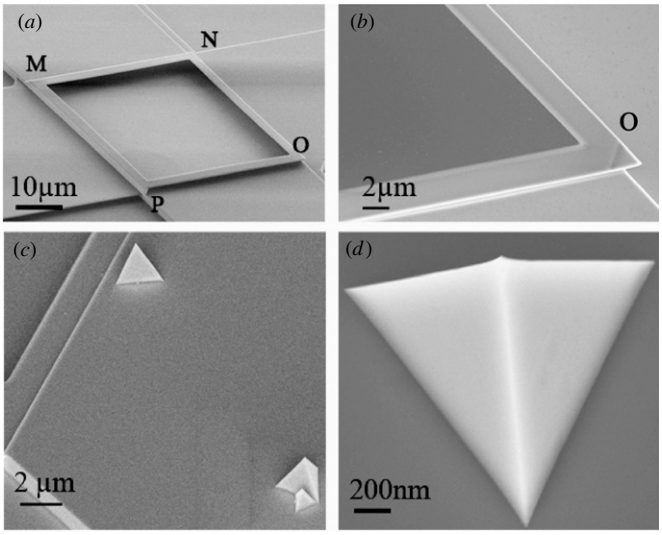

Figure 7. (*a*) SEM image of the final anisotropic structures. The tetrahedron is at the corner '*O*' of this structure. (*b*) Zoom in image of the O-corner showing the tetrahedron covered with oxide. (*c*, *d*) Tetrahedra released from the oxide frame after HF. A smaller tetrahedron formed at the corner P is also observed by the tetrahedron formed at the O-corner.

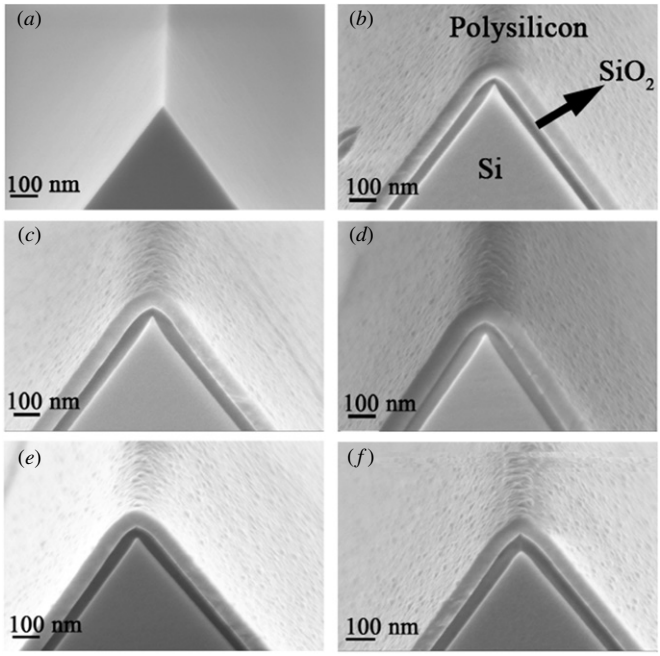

Figure 9. SEM images of the ⟨1 1 1⟩ ridges (*a*) before oxidation. (*b*) After dry oxidation at 950 °C, (*c*) 1000 °C, (*d*) 1050 °C, (*e*) 1100 °C, (*f*) and 1150 °C.

(figure 9(*f*)). It is concluded that 1100 °C is the optimum temperature, which leaves the ⟨1 1 0⟩ ridge without excessive sharpening or rounding.

Despite the former 'optimized' result, the 350 nm LOCOS needed to reveal the last face does not lead to the mathematically correct tetrahedral shape. In the tetrahedron of figure 7(*d*) a slight sharpening can be observed at one of the tips, which is not noticeable at the other tips. We assume that this imperfect tip is the A-tip as shown in figure 1(*b*).

3.2. Uniformity

The size of the tetrahedra is controlled by two etch processes: The retraction length *X* in figure 4 and the etch rate of silicon in the ⟨1 1 1⟩ direction. The etch rate of silicon nitride in 50% HF is very close to 1.20 μm min^{-1} and, according to our microscopic inspection of the wafers, quite homogeneous (the optical instrument limits the measurement of the retraction length to about 100 nm; this is also the variation we find in our measurements). The reproducibility of the Si⟨1 1 1⟩ etch rate has not been systematically studied; in our experience the reproducibility is within experimental errors. The uniformity of the process over a wafer is indicated in figures 8(*a*)–(*c*): the specimens are from different parts of the wafer. They seem to be quite similar in size. The uniformity therefore is better than 5%.

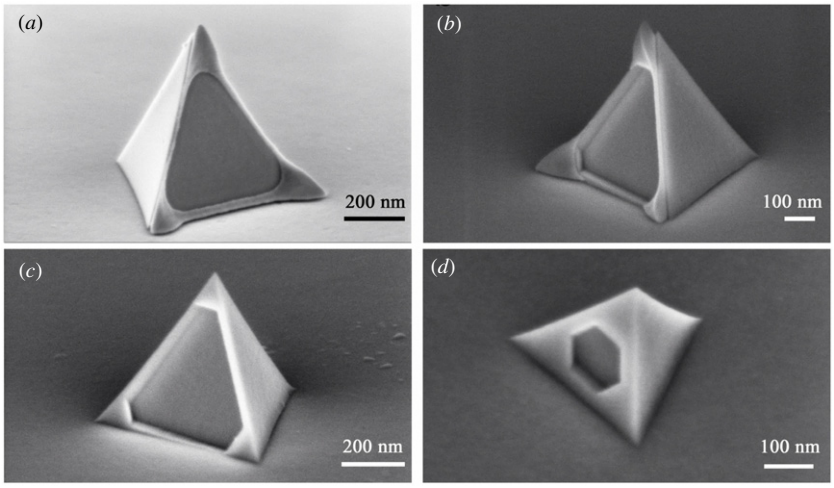

Figure 8. SEM images of tetrahedral structures after selective modification of top face. (*a*) After release using HF but without an additional TMAH etch, (*b*) after release while the first face is patterned in TMAH, (*c*) the released structure of b after stripping the nitride mask, (*d*) structure released from the P-corner as marked as in figure 7, after stripping the nitride mask.

4. Conclusion

In conclusion, we fabricated silicon tetrahedral structures bound by ⟨1 1 1⟩ faces out of Si⟨1 1 1⟩ wafers. The special aspect of this process is that one of the tetrahedral faces is oriented parallel to the wafer surface. We have shown that the side of the tetrahedron parallel to the wafer can be modified by corner lithography. Due to dependence of the thermal oxidation of silicon on stress the tetrahedra are not yet perfect: the tips tend to be slightly sharpened. We find that the process yields tetrahedra of uniform size: the variation in size is less than 5%.

Acknowledgments

The authors wish to thank Freiburg Institute for Advanced Studies (FRIAS) for funding the project.

References

[1] Sadler D J, Garter M J, Ahn C H, Koh S and Cook A L 1997 Optical reflectivity of micromachined-oriented silicon mirrors for optical input-output couplers *J. Micromech. Microeng.* **7** 263–9
[2] Trupke M *et al* 2006 Pyramidal micromirrors for microsystems and atom chips *Appl. Phys. Lett.* **88** 071116
[3] Kim J, Cho D and Muller R S 2001 Why is (1 1 1) silicon a better mechanical material for MEMS *Proc. Transducers 2011: 11th Int. Conf. on Solid-State Sensors and Actuators (Munich, Germany June 2001)* pp 662–5
[4] Zhang Z, Keys A S, Chen T and Glotzer S C 2005 Self-assembly of patchy particles into diamond structures through molecular mimicry *Langmuir* **21** 11547–51
[5] Chen E R, Engel M and Glotzer S C 2010 Dense crystalline dimer packings of regular tetrahedra *Discrete Comput. Geom.* **44** 253–80
[6] Damasceno P F, Engel M and Glotzer S C 2011 Crystalline assemblies and densest packings of a family of truncated tetrahedra and the role of directional entropic forces *ACS Nano* **6** 609–14
[7] Haji-Akbari1 A, Engell M, Keys A S, Zheng X, Petschek R G, Palffy-Muhoray P and Glotzer S C 2009 Disordered, quasicrystalline and crystalline phases of densely packed tetrahedra *Nature* **462** 773–7
[8] Barret C A, Dickinson C, Ahmed S, Hantschel T, Arstila K and Ryan K M 2009 The evolution of pseudo-spherical silicon nanocrystals to tetrahedra, mediated by phosphonic acid surfactants *Nanotechnology* **20** 275605
[9] Berenschot J W, Tas N R, Jansen H V and Elwenspoek M 2009 Chemically anisotropic single-crystalline silicon nanotetrahedra *Nanotechnology* **20** 475302
[10] Elwenspoek M and Jansen H V 1998 *Silicon Micromachining* (Cambridge: Cambridge University Press)
[11] Rusu C *et al* 2001 Direct integration of micromachined pipettes in a flow channel for single DNA molecule study by optical tweezers *J. Microelectromech. Syst.* **10** 238–46
[12] Holly R and Hingerl K 2006 Fabrication of silicon vertical taper structures using KOH anisotropic etching *Microelecton. Eng.* **83** 1430–3
[13] Holly R, Hingerl K, Merz R and Hudek P 2007 Fabrication of silicon 3D taper structures for optical fibre to chip interface *Microelectron. Eng.* **84** 1248–51
[14] Sarajlic E, Yamahata C and Fujita H 2007 Towards wet anisotropic silicon etching of perfect pyramidal pits *Microelectron. Eng.* **84** 1419–22
[15] Alavi M, Buttgenbach S, Schumacher A and Wagner H J 1992 Fabrication of microchannels by laser machining and anisotropic etching of silicon *Sensors Actuators* A **32** 299–302
[16] Tixier-Mita A, Mita Y and Fujita H 2003 A simple, robust and controllable nano-structures fabrication technique using standard silicon wafers *Proc. Transducers '03* pp 250–3
[17] Oosterbroek R E, Berenschot J W, Jansen H V, Nijdam A J, Pandraud G, Van Den Berg A and Elwenspoek M C 2000 Etching methodologies in ⟨1 1 1⟩-oriented silicon wafers *J. Microelectromech. Syst.* **9** 390–8
[18] Zhao Y, Berenschot J W, de Boer M J, Jansen H V, Tas N R, Huskens J and Elwenspoek M C 2008 Fabrication of a silicon oxide stamp by edge lithography reinforced with silicon nitride for nano imprint lithography *J. Micromech. Microeng.* **18** 064013
[19] Zhao Y, Berenschot J W, Jansen H V, Tas N R, Huskens J and Elwenspoek M C 2009 Sub-10 nm silicon ridge nanofabrication by advanced edge lithography for NIL applications *Microelectron. Eng.* **86** 832–5
[20] Zhao Y, Berenschot J W, Jansen H V, Tas N R, Huskens J and Elwenspoek M C 2009 Multi-silicon ridge nanofabrication by repeated edge lithography *Nanotechnology* **20** 315305
[21] Zhao Y, Jansen H V, de Boer M, Berenschot E, Bouwes D, Girones M, Huskens J and Tas N 2010 Combining retraction edge lithography and plasma etching for arbitrary contour nanoridge fabrication *J. Micromech. Microeng.* **20** 095022
[22] Allongue P, Kosta-Kieling V and Gerischer H 1993 In situ observation of the etching of n-Si(1 1 1) in NaOH solutions *J. Electrochem. Soc.* **140** 1009
[23] Elwenspoek M 1993 *J. Electrochem. Soc.* **140** 2075–80
[24] Schnakenherg U, Benecke W and Lange P 1991 TMAHW etchant for silicon micromachining *Tech. Digest of Transducers 91 (San Francisco, USA, June)* pp 815–8
[25] Tabata O, Asahi R, Funabashi H, Shimaoka K and Sugryama S 1992 Anisotropic etching of silicon in TMAH solutions *Sensors Actuators* **34** 51–7
[26] Koelmans W W, Peters T, Berenschot E, de Boer M J, Siekman M H and Abelmann L 2012 Cantilever arrays with self-aligned nanotips of uniform height *Nanotechnology* **23** 135301
[27] Jansen H V, de Boer M J, Unnikrishnan S, Louwerse M C and Elwenspoek M C 2009 Black silicon method X. A review on high speed and selective plasma etching of silicon with profile control: an in-depth comparison between Bosch and cryostat DRIE processes as a roadmap to next generation equipment *J. Micromech. Microeng.* **19** 033001
[28] Berenschot E, Tas N R, Jansen H V and Elwenspoek M 1998 3D-nanomachining using corner lithography *Proceedings of the 3rd IEEE Int. Conf. on Nano/Micro Engineered and Molecular Systems (Sanya, China)* pp 729–32